Society For Biomaterials

Influence of surface topography and surface physicochemistry on wettability of zirconia (tetragonal zirconia polycrystal)

Akio Noro,[1,2] Morio Kaneko,[3] Isao Murata,[3] Masao Yoshinari[1]

[1]Division of Oral Implants Research, Oral Health Science Center, Tokyo Dental College, Mihama-ku, Chiba 261-8502, Japan
[2]Division of General Dentistry, Tokyo Dental College Chiba Hospital, Mihama-ku, Chiba 261-8502, Japan
[3]Japan Institute for Advanced Dentistry, Minato-ku, Tokyo 105-0014, Japan

Received 12 March 2012; revised 30 June 2012; accepted 25 September 2012
Published online in Wiley Online Library (wileyonlinelibrary.com). DOI: 10.1002/jbm.b.32846

Abstract: Surface modification technologies are available for tetragonal zirconia polycrystal (TZP) to enhance its bioactivity and osseointegration capability. The surface wettability of an implant material is one of the important factors in the process of osseointegration, possibly regulating protein adsorption, and subsequent cell behavior. The aim of this study was to clarify the effect of topographical or physicochemical modification of TZP ceramics on wettability to determine the potential of such treatment in application to implants. Several types of surface topography were produced by alumina blasting and acid etching with hydrofluoric acid; surface physicochemistry was modified with oxygen (O_2) plasma, ultraviolet (UV) light, or hydrogen peroxide treatment. The obtained specimens were also subjected to storage under various conditions to evaluate their potential to maintain superhydrophilicity. The results showed that surface modification of surface topography or physicochemistry, especially of blast/acid etching as well as O_2 plasma and UV treatment, greatly increased the surface wettability, resulting in superhydrophilicity. X-ray photoelectron spectroscopy revealed that a remarkable decrease in carbon content and the introduction of hydroxyl groups were responsible for the observed superhydrophilicity. Furthermore, superhydrophilicity was maintained, even after immersion in an aqueous solution, an important consideration in the clinical application of this technology. © 2012 Wiley Periodicals, Inc. J Biomed Mater Res Part B: Appl Biomater 00B:000–000, 2012.

Key Words: zirconia, hydrophilicity, surface modification, oxygen plasma, ultraviolet light

How to cite this article: Noro A, Kaneko M, Murata I, Yoshinari M. 2012. Influence of surface topography and surface physicochemistry on wettability of zirconia (tetragonal zirconia polycrystal). J Biomed Mater Res Part B 2012:00B:000–000.

INTRODUCTION

In the field of dentistry, zirconia, and especially tetragonal zirconia polycrystal (TZP), have shown outstanding mechanical, biocompatible, and esthetic performance, offering superiority over titanium (Ti) implants in terms of discoloration and hyper-responsiveness.[1–3] At the tissue level, TZP was found to be as biocompatible as Ti.[4,5] Rough-surfaced TZP implants yielded a greater removal torque value than control implants, although not to the level of that observed in Ti implants.[6] Although various surface-roughening technologies are available to enhance the bioactivity and osseointegration capability of Ti, little is known about the clinical findings on TZP implants. On *in vivo* study, the osseointegration capability and durability of TZP implants has been reported to be similar to that of Ti implants in a number of animal experiments, indicating its suitability as an implant material.[7,8] Differences in alumina-toughened zirconia surface topography showed no significant effect on proliferation rate.[9] Roughened TZP was an appropriate substrate for proliferation and spreading of osteoblastic cells.[10] Acid-etched TZP improved cell proliferation significantly during the first days of culture, but not attachment or adhesion strength on *in vitro* study.[8]

The vital reaction to a dental implant will be affected by the surface topography and surface physicochemistry of the material used. Surface topography has a marked effect on cell behavior. Moreover, protein adsorption and subsequent cell behavior will depend on surface physicochemistry, especially surface energy (wettability) and electric charge.[11,12] Many *in vitro* studies have investigated the relationship between the hydrophilicity of a material surface and cell adhesion.[13–17] High surface wettability, which means high surface energy, is generally reported to promote greater cell adhesion than low surface energy.

Correspondence to: M. Yoshinari; e-mail: yosinari@tdc.ac.jp
Contract grant sponsor: Oral Health Science Center Grant hrc7 and hrc8 from Tokyo Dental College, a "High-Tech Research Center" Project for Private Universities: Matching Fund Subsidy from MEXT (Ministry of Education, Culture, Sports, Science and Technology) of Japan, 2006–2010 and 2010–2012.
Contract grant sponsor: Japan Society for the Promotion of Science (Grant-in-Aid for Scientific Research); contract grant numbers: B:18390524 and 18659581

In cell–material interactions, protein adsorption is one of the first things to take place at the solid/liquid interface when a material is exposed to a bodily fluid or culture media. Fibronectin (Fn), a cell adhesion protein, and albumin (Alb), a cell adhesion-inhibiting protein, are both included in serum used for cell culture. This suggests that the competitive adsorption behavior of these proteins should be analyzed for more insight into the relationship between protein adsorption and cellular attachment.[18] In earlier studies, we evaluated the adsorption behavior of Fn and Alb in both individual and competitive modes and the initial attachment of osteoblasts on surfaces with a wide range of wettability. The results confirmed that superhydrophilic surfaces increased Fn adsorption and that the more hydrophilic the surface, the more cells adhered during the initial stage of osseointegration. Cell spread was also greater on hydrophilic surfaces than on hydrophobic surfaces.[14,15]

Wettability and surface energy are affected by both surface topography and physicochemistry. Cold plasma treatment, including glow discharge,[14,15,19–21] and ultraviolet (UV) light irradiation[22,23] have been proposed as a means of modifying wettability. Chemical treatment, such as acid etching, may also enhance the wettability of TZP surfaces by eliminating adsorbed impurities such as hydrocarbon from the atmosphere.[23] Thus, surface wettability may be influenced not only by surface topography but also surface physicochemistry. Therefore, the aim of this study was to clarify the effect of topographical or physicochemical modification of TZP ceramics on wettability to determine the potential of such treatment in application to implants. The obtained specimens were also subjected to storage under various conditions to evaluate their potential to maintain superhydrophilicity.

MATERIALS AND METHODS

Surface treatment

TZP (TZ-3YB-E, Tosoh, Japan) sintered at 1350°C for 2 h in air was used in this study. TZP disks 13 mm in diameter and 0.5 mm in thickness were first obtained using a cutting machine.

The obtained disks were then modified as follows (Table I): mirror polished with colloidal silica (MS) specimens, prepared using a machine (Ecomet 3, Buehler, Lake Bluff, IL) which created the required surfaces by first polishing with 9- and 3-μm diamond and then 0.6-μm colloidal silica; grit-blasted specimens, prepared by perpendicular grit blasting from a distance of 10 mm with 25-, 50-, or 150-μm alumina particles at 0.4 MPa air pressure; and acid-etched specimens (designated SB150E in Table I) prepared by etching SB150 with 47% hydrofluoric acid (HF) at room temperature for 15 min. All types of specimen were then ultrasonically cleaned with acetone and distilled water.

The surface-modified TZP disks were also subjected to the following types of physicochemical treatment, apart from the control specimens (AS), which were stored in air only for 10 min immediately after cleaning (Table I); Oxygen (O_2) plasma specimens, prepared with a plasma-surface modification apparatus (VEP-1000, ULVAC, Japan). Briefly, the specimens were introduced into the chamber of the apparatus and exposed to O_2 low-energy plasma treatment (200 W; 1.5 Pa; gas flow rate, 50 sccm) at room temperature for 10 min; UV light specimens, subjected to UV radiation using a UV ozone cleaner (PC440, Bioforce Nanosciences, Sweden) for 2 h. This equipment creates UV radiation with a total power of 19 mW/cm^2 and excitation wavelengths of 185 and 254, which correspond to UV-C, and 365 nm, which corresponds to UV-A; hydrogen peroxide (H_2O_2) specimens, prepared by immersion in 150 m*M* H_2O_2 solution at 60°C for 1 day.

TABLE I. Surface Treatments Affecting Topography or Physicochemistry

Code	Treatment
Surface topography	
MS	Mirror polished with colloidal silica
SB25	Blasted with 25 μm alumina
SB50	Blasted with 50 μm alumina
SB150	Blasted with 150 μm alumina
SB150 + HF	Etched SB150 with HF (46%) for 15 min
Surface physicochemistry	
AS (control)	Stored in air for 10 min
O_2 plasma	Treated with oxygen plasma (1.5 Pa, 200 W) for 10 min
UV	Treated with ultraviolet radiation (19 mW/cm^2) for 2 h
H_2O_2	Immersed in 150 m*M* H_2O_2 solution (60°C) for 1 day

Surface microstructure and surface roughness

The surface microstructure of the specimens was observed using a field emission scanning electron microscope (JSM-6340F; JEOL, Japan) at an accelerating voltage of 15 kV.

The surface roughness with 2-D analysis was evaluated using a profilometer (Surfcom 130A, Accretech, Tokyo, Japan). The arithmetical mean surface roughness (Ra) was determined under these conditions with a cut-off value of 0.8 mm, measurement length of 4.0 mm, and measurement speed of 0.6 mm/s. Three samples of each treatment were measured. Analyses of 3-D surface characteristics were also performed using an electron beam 3-D surface roughness analyzer (ERA-8900FE; Elionix, Tokyo, Japan) at an accelerating voltage of 15 kV. To obtain a multiscale characterization of the surface topography, images were acquired in a dimensional range of 60 μm × 45 μm and a Gaussian filter of 60 μm × 45 μm as recommended by previous reports.[24,25] The following surface parameters were considered:

Sa (μm): average roughness; average height deviation from a mean plane within the area measuring area (correspond to 2-D Ra).

Sdr: developed interfacial area ratio; additional surface area created by roughness compared with that of totally flat plane (no correspond to 2-D measurement).

Surface wettability

The surface wettability of the samples was characterized by contact angle measurement with double-distilled water (DW) using a contact angle meter (Phoenix α, Meiwa-forces,

TABLE II. Storage Conditions (SB150 + HF)

Code	Condition
Air	Air
DW	Distilled water
NaCl	0.9% NaCl solution
NaOH	3% NaOH solution
Eth	99% ethanol

Japan). Measurements were made at three different locations on each sample (five of each type of surface topography) at 15 s after application of the droplet. The volume of the drop was maintained at 4 μL. Before measuring, specimens were gently blown with compressed nitrogen for approximately 30 s.

The durability of the surface wettability of the SB150 + HF specimens with each type of physicochemical modification was also evaluated by contact angle measurement at room temperature over 21 days under various storage conditions, as shown in Table II.

Surface free energy

The surface free energy value of the MS specimens with each type of physicochemical modification was determined by measurement of the contact angles of two test liquids (DW and Di-iodomethane) and plots of the Owens-Wendt equation. Total surface free energy (γ^{total}), including the dispersion component (γ^{d}) and polar component (γ^{p}), was calculated.

XPS analysis

An X-ray photoelectron spectroscopy (XPS) analysis (AXIS-ULTRA, KRATOS Analytical, GBR) was performed to determine the composition of the outermost surface and chemical shift, using an X-ray source of Al Kα (monochromator), 15 kV and 15 mA to determine the intensity of Zr 3d, C 1s, and O 1s. The binding energy of each spectrum was calibrated with a C 1s of 285.0 eV.

Statistical analysis

The statistical significance of the data was assessed by an analysis of variance, followed by the Scheffe test for multiple comparisons between pairs at $p = 0.05$.

RESULTS

Surface microstructure and surface roughness

Surface microstructures are shown in Figure 1. The MS specimens showed a generally flat surface with a small number of pits. Surface roughness increased with increase in size of the alumina particles used for blasting. The SB150 + HF specimens showed a fine texture with a comparatively large configuration.

Figure 2 shows surface roughness of Ra values with 2-D analysis and Sa values with 3-D analysis (a) and Sdr with 3-D surface analysis (b). Both Ra and Sa values showed an increase in the order of MS, SB50, SB150, and SB150E. Though the Sdr values showed the same tendency as the Sa values, no clear difference in Sdr values was observed between SB25, SB50, and SB150. However, significantly higher Sdr values were observed in the SB150E than in the SB150 specimen.

Surface wettability

Figure 3 shows an example of top and cross-sectional views of a droplet of water on SB150 and SB150 + HF under control conditions (AS). The SB150 specimen had a comparatively large contact angle of 55°, whereas, surprisingly, superhydrophilicity with a contact angle of 0° was observed on the SB150 + HF specimen.

Figure 4 shows the water contact angles of the specimens with each type of surface topography and physicochemistry. These values were obtained at after blast or blast and acid etching. From a topographical point of view (see

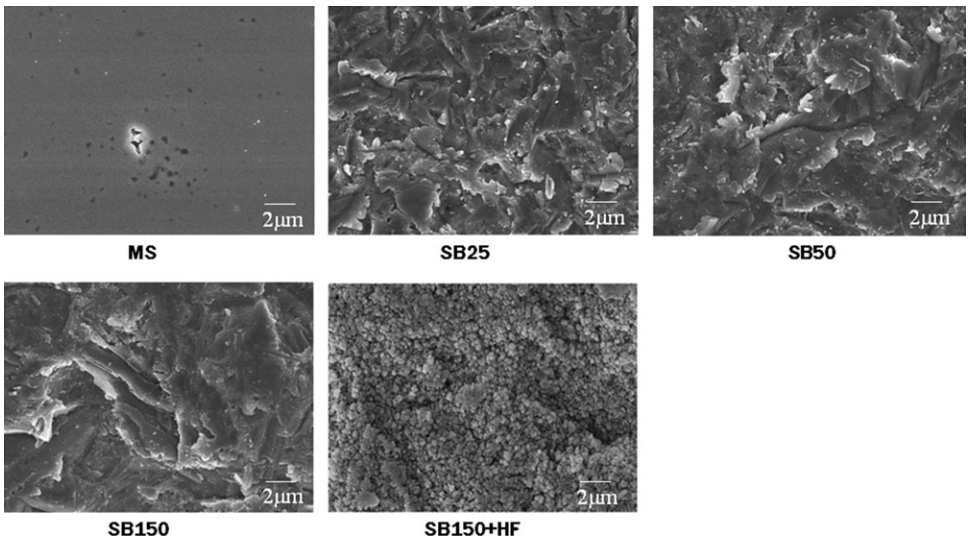

FIGURE 1. Surface microstructures of surface-treated specimens.

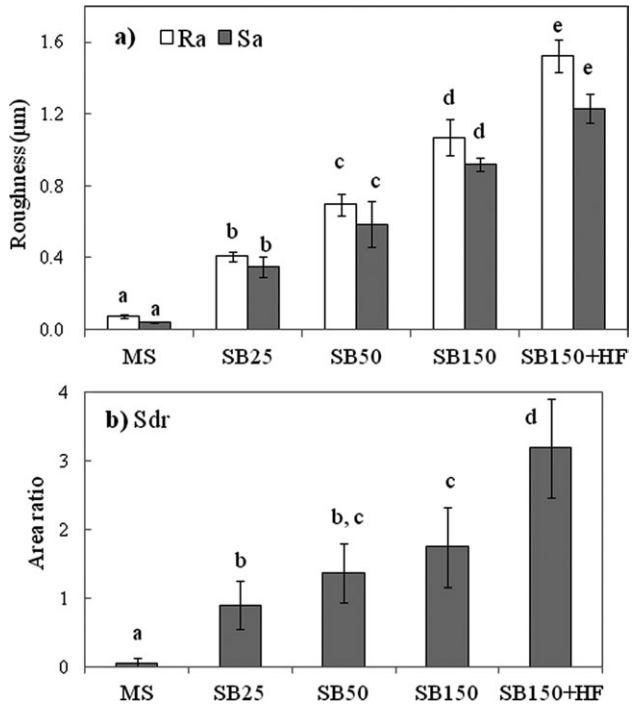

FIGURE 2. (a) Surface roughness of Ra values with 2-D analysis and Sa values with 3-D analysis and (b) developed interfacial area ratio (Sdr) with 3-D surface analysis. Identical letter shows no significant difference on each Ra, Sa, and Sdr values.

AS inset in Figure 3), no large differences were observed in contact angle among the specimens, apart from in the SB150 + HF specimens, which showed superhydrophilicity, with a contact angle of almost 0°. From a physicochemical point of view, the contact angle in the O_2 plasma, UV, and H_2O_2 specimens decreased in comparison with that of the AS specimens, with that in the O_2 plasma specimens, in particular, indicating superhydrophilicity under all types of surface topography. The SB150 + HF specimens showed superhydrophilicity, with a contact angle of almost 0°, regardless of type of physicochemical treatment.

Durability of surface wettability

Figure 5 shows change in contact angle with passage of time in the SB150 + HF specimens with each type of sur-

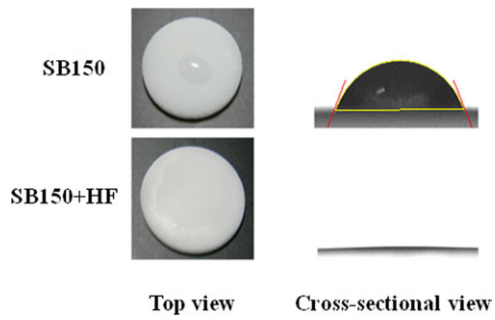

FIGURE 3. Top and cross-sectional views of water droplet in AS specimens (storage in air only for 10 min). [Color figure can be viewed in the online issue, which is available at wileyonlinelibrary.com.]

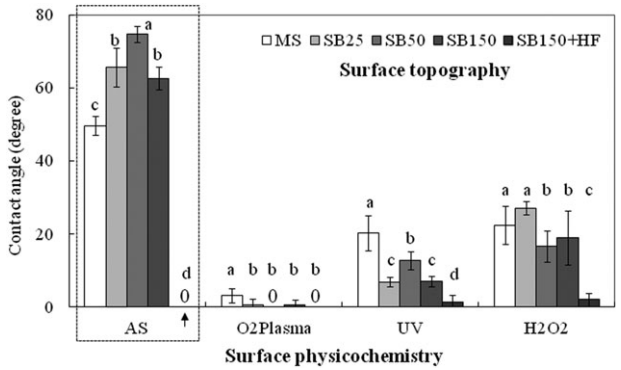

FIGURE 4. Water contact angle in specimens by type of surface topography and physicochemistry after storage in air for 10 min. Identical letter indicates no significant difference between each type of surface physicochemistry.

face physicochemistry. Contact angle showed an increase in all specimens with time under storage in air. On the other hand, hydrophilicity was maintained under all other storage conditions, including DW.

Surface free energy

Figure 6 shows γ^{total}, γ^{d}, and γ^{p} after storage in air for 10 min in the MS specimens with each type of physicochemical modification. Total surface energy was larger in the O_2 plasma, UV, and H_2O_2 specimens than in the AS specimens, especially in the O_2 plasma specimens. These results mainly corresponded to an increase in γ^{p}.

XPS analysis

Figure 7 shows a summary of the carbon content (at %) on the outermost surface of the TZP discs. A comparison based on surface topography is shown in Figure 6(a): carbon content showed a remarkable decrease in the SB150 + HF specimens in comparison with the others. Figure 6(b) shows a comparison based on surface physicochemistry: carbon content in the O_2 plasma and UV specimens was smaller than that in the AS or H_2O_2 specimens after storage in air for 10 min. In addition, carbon content in the air 10 min specimens was lower than that observed in Air21d specimens.

A typical O 1s spectrum of the TZP disks is given in Figure 8(a). Three peaks were defined as ZrO_2 at around 530.2 eV, OH(a) at around 531.5 eV and OH(b) at around 532.5 eV by deconvoluting the O 1s peak based on the Ti oxide according to the previous reports. Here, OH(a) and OH(b) indicate acidic hydroxyl and basic hydroxyl groups, respectively.

Figure 8(b) shows percentage areas of OH(a) and OH(b) depending on surface topography. Percentage areas of OH(a) showed a decrease in the order of MS, SB150 + HF, and SB150. However, the largest percentage area of OH(b) was observed in the SB150 + HF specimens.

The percentage areas of OH(a) and OH(b) in the SB150 + HF specimens with each type of physicochemical modification and storage condition are shown in Figure 8(c,d),

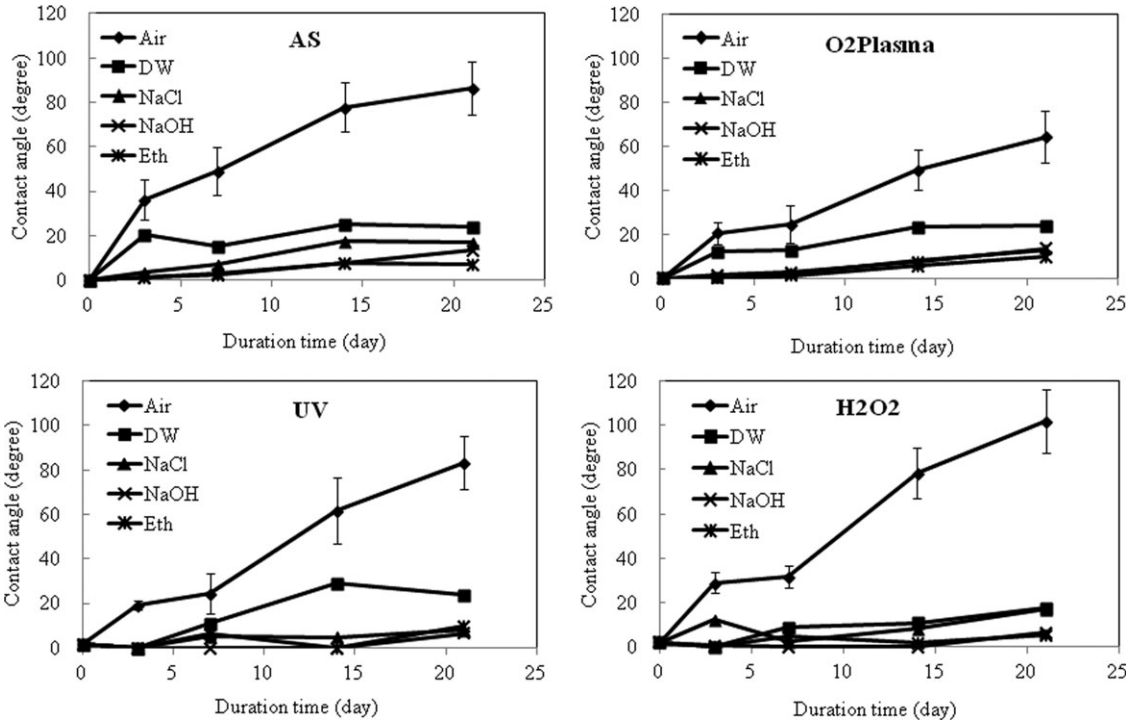

FIGURE 5. Durability of surface wettability in SB150 + HF under each storage condition.

respectively. No significant difference was observed in OH(a) among specimens between each type of surface physicochemistry. However, the O_2 plasma specimens showed a higher percentage area of OH(b) than the others. Specimens stored in air for 21 days showed the smallest percentage areas of both OH(a) and OH(b).

DISCUSSION

In this study, the surface topography of TZP disks was modified by various types of treatment, including mirror polishing, blasting with different sizes of alumina particle, and etching with HF. The results of the wettability tests revealed a dramatic decrease in contact angle in the SB150 + HF specimens after storage in DW for 10 min, indicating superhydrophilicity, whereas it was more than 50° in the other surface topographies (Figure 3). In general, Ti constantly adsorbs organic impurities such as hydrocarbons from the atmosphere. This leads to an increase in hydrophobicity, which is referred to as an aging phenomenon.[26] It has also been reported that the atomic percentage of carbon reaches 50 at % in hydrophobic Ti surfaces stored in air.[27]

In this study, we used the TZP that were sintered at 1350°C in air, because this kind of TZP was widely applied in the dental field. However, a low mechanical property of conventional TZP was reported, and thus, zirconia with high strength is desirable to ensure the durability under the clinical performance such as HIP/alumina toughened zirconia (ATZ).[28–30]

A negative physical characteristic of Y-TZP was also reported as low temperature degradation LTD,[30–32] and may result in a significant reduction in the strength and toughness of Y-TZP[33] as the main clinical drawbacks over a long term period. Surface treatment such as grinding, sandblasting and acid-etched should be utilized to enhance the osseointegration when the zirconia is used for the implant body. Such surface treatment may induce the phase transformation, from tetragonal to monoclinic zirconia, as well as superficial microcracks, resulting in change in its mechanical properties in terms of both static and fatigue strength.[33–35]

We expressed superhydrophilicity, with a contact angle of almost 0°, because it is often noted that the superhydrophilic substrate refers to one on which water/liquid spreads to zero or nearly zero contact angle.[36] It should be recognized that the term superhydrophilic materials only refers to those textured and/or structured materials (rough and/

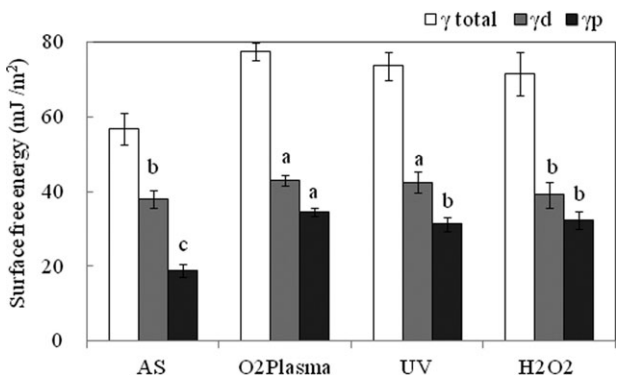

FIGURE 6. Total surface free energy (γ^{total}), dispersion component (γ^{d}), and polar component (γ^{p}) in MS specimens with each type of surface physicochemistry after storage in air for 10 min. Identical letter indicates no significant difference in γ^{d} or γ^{p}.

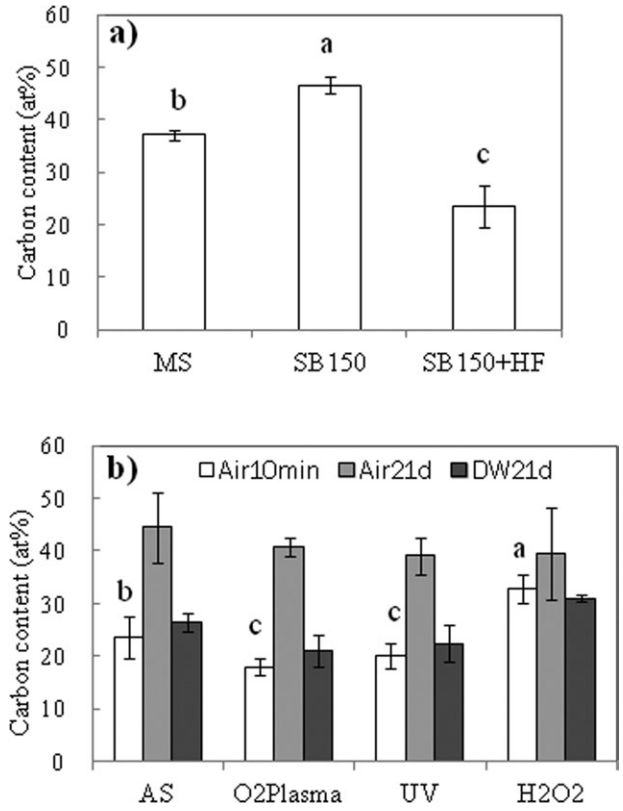

FIGURE 7. Carbon content on outermost surface of TZP discs by XPS analysis. (a) Comparison by surface topography after storage in air for 10 min. (b) Comparison by surface physicochemistry of SB150 + HF specimens under each storage condition. Air10min: after storage in air for 10 min, Air21d: after storage in air for 21 days, and DW21d: after storage in distilled water for 21 days. Identical letter indicates no significant difference (multiple comparisons were performed on air 10 min in days).

or porous) having a surface roughness factor (as defined in the Wenzel equation) larger than one, $r > 1$, on which water (liquid) spreads completely.[37]

It is widely accepted that the importance of 3-dimensional (3-D) surface characterization in addition to conventional 2-D roughness (Ra) in evaluating cellular response to change in surface topography has been noted.[24,25] In the guidelines on surface characterization, Wennerberg and Albrektsson emphasized the importance of multiple roughness parameters. They noted that surface topography cannot be characterized well with only one parameter, because one surface may have the same height deviation but differ in spatial distribution when compared with another. They also recommend multiscale measurements with proper filtering procedures to exclude errors of form and waviness. In this study, significantly higher Sdr values by 3-D analysis were observed in the SB150E than in the SB150 specimen, indicating that both micro- and nanotopographies had been produced on the SB150E surfaces.

The increase in superhydrophilicity in the SB150 + HF specimens observed in this study may be explained as follows. First, acid etching may have served to clean the surface, decreasing the likelihood of hydrocarbon being absorbed during storage in air. This phenomenon was confirmed by the XPS analysis [Figure 6(a)], which showed a remarkable decrease in carbon content in the SB150 + HF specimens. Second, superhydrophilicity may have been enhanced by the larger surface area created by blast and acid etching. This phenomenon has been described in the Wenzel model,[38] which predicts that the contact angle on a flat surface, which is $\theta < 90^\circ$, will decrease if the surface is roughened. That is, $\cos \theta_w = r \cos \theta$: where θ is the contact angle on a flat surface of the same nature, θ_w is the apparent contact angle, and r is the surface roughness factor defined as the ratio of the actual surface over the surface as measured on the plane of the interface (in general, $r > 1$, and $r = 1$ for flat surfaces). In this study, the SB150 + HF specimens had a nanostructure created by acid etching on an uneven surface created by large-grit blasting (Figure 1). The resulting increase in surface area appears to have enhanced hydrophilicity. It is considered that other grit blasting with acid etching procedure might show same superhydrophilicity with same mechanism as increase in superhydrophilicity in the SB150 + HF specimens.

From a physicochemical point of view, the contact angle decreased in the O_2 plasma, UV, and H_2O_2 specimens compared with in the AS specimens, with the O_2 plasma specimens, in particular, showing superhydrophilicity under all types of surface topography.

Cold plasma-surface modification, including plasma treatment with various gases, is suitable for changing the surface physicochemistry.[12] Wei et al.[14] investigated the effects of surface modification by plasma polymerization with hexamethyldisiloxane followed by O_2 Plasma treatment. In their study, the water contact angle of sample surfaces varied from 106° (hydrophobicity) to almost 0° (superhydrophilicity), with O_2 functional groups being introduced during O_2 Plasma treatment. Another study on Ti found that hydroxylation of the TiO_2 substrate by exposure to O_2 Plasma was similar to water photo-oxidation by exposure to UV irradiation. And the hydroxylated TiO_2 substrate was constructed in the form of Ti–OH via oxidation by O_2 Plasma and nucleophilic attack of H_2O molecules present in the atmosphere.[39] O_2 plasma treatment of TZP surfaces is expected to decrease hydrocarbon content, and creating O_2 functional groups such as hydroxyl groups. These phenomena were confirmed by XPS analysis in this study (Figures 7 and 8).

In this study, TZP surfaces treated with UV also showed superhydrophilicity. UV light-induced superhydrophilicity of TiO_2 was discovered in 1997.[40] In this model, UV light irradiation creates surface O_2 vacancies at bridging O_2 sites. Wetting is caused by surface physicochemistry alteration by TiO_2 photocatalytic activity in association with the photocatalytic removable of hydrocarbon from the surface.[41,42] In the case of Ti, a UV light energy of greater than 3.2 eV, corresponding to a wavelength of less than 387 nm, is needed to induce TiO_2 (anatase) photocatalytic activity to excite an electron from the valence band to the conduction band.[40] Another semiconducting photocatalyst material, ZrO_2, also shows superhydrophilicity, like TiO_2.[43,44] The band gap of

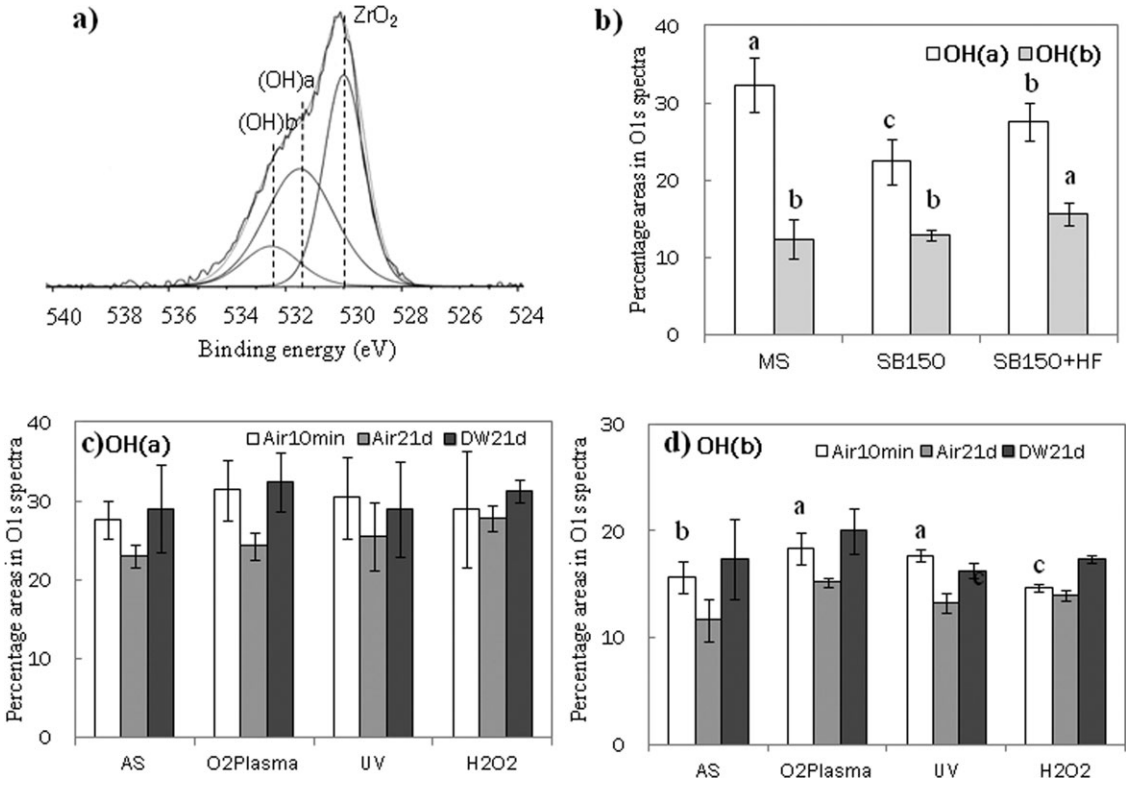

FIGURE 8. O 1s spectra on outermost surface of TZP disks under XPS analyses. (a) Typical O 1s spectrum and (b–d) percentage areas of OH(a) and OH(b) in O 1s spectra. (b) Comparison in surface topography after storing in air for 10 min. (c and d) Comparison in surface physicochemistry of SB150 + HF specimens with various storage conditions (c: OH(a), d: OH(b)). Air10min: after storing in air for 10 min, Air21d: after storing in air for 21 days, and DW21d: after storing in distilled water for 21 days. Identical letter shows no significant difference (multiple comparisons were performed on the Air10min in days).

ZrO_2 is 5.82 eV, which corresponds to an approximately 213 nm of wavelength. The equipment used to generate UV irradiation in this study used excitation wavelengths of 185, 254, and 365 nm, among which the lower wavelengths were predicted to produce photocatalytic activity.

H_2O_2 treatment has been used to introduce Ti–OH groups onto Ti surfaces to enhance wettability.[45,46] In this study, this resulted in moderate enhancement of hydrophilicity. Further study is necessary, however, to clarify the optimum concentration and temperature at which the H_2O_2 solution should be applied.

Durability of surface wettability is an important consideration in the practical application of this technology in a clinical setting. The water contact angle in the SB150 + HF specimens showed a rapid increase over time, reaching 85° at 21 days in air. On the other hand, hydrophilicity was maintained in all specimens, including those subjected to blast or acid etching, with storage in an aqueous solution (DW, 0.9% NaCl, or 3% NaOH) or ethanol. These phenomena were confirmed by XPS analysis [Figure 6(b)], and a relatively low level of carbon content of the specimens in aqueous solutions compared with those stored in air. The potential to maintain surface wettability during storage in an aqueous solution is important from a clinical point of view.

The observed decrease in contact angle by physicochemical surface treatment was supported by the results of the XPS analysis: the carbon content showed a remarkable decrease and amount of hydroxyl groups an increase in the O_2 plasma, and UV specimens in comparison with in the AS specimens, apart from SB150 + HF.

There are two kinds of OH group on Ti outermost surfaces, OH(a) and OH(b), negatively charged acidic hydroxyl groups and positively charged basic hydroxyl groups, respectively, playing an important role in protein adsorption.[47] Feng et al.[48] also showed that at the initial stage of the cell culture the OH(b) groups were consumed in great amounts due to the involvement of the chemical interaction between the osteoblasts and the Ti surfaces, indicating that the (OH)b groups probably played a more important role than the (OH)a groups in the bioactivity of Ti. In this study, a greater increase in OH(b) was observed in the O_2 plasma specimens than in the AS, UV, or H_2O_2 specimens [Figure 8(d)], despite no apparent differences between them in terms of basic hydroxyl OH(a) groups [Figure8 (c)]. The underlying mechanism of this phenomenon, however, remains to be revealed.

Surface energy affects cell behavior, with cells spreading and attaching more easily on surfaces with high surface energy. Earlier studies found that the greater the surface roughness, the higher the surface energy and the more the number of surface hydroxyl groups, resulting in greater numbers of adhered osteoblasts and higher cell activity.[49,50] In this study, the O_2 plasma, UV, and H_2O_2 specimens

showed an increase in total surface energy compared with the AS specimens (Figure 5). The dispersion component (γ^d) in surface energy was similar among the surface-treated groups, whereas polar component (γ^p) was significantly different. The γ^p values showed a larger increase in the O_2 plasma specimens than in the UV or H_2O_2 specimens. It was reported that γ^p influenced the behavior of osteoblasts on Ti surfaces more strongly than γ^d, which was attributed to the fact that interaction between cells and Ti is mainly governed by polar force.[31] A higher γ^p leads to higher interaction energy. Hence, O_2 plasma treatment is expected to enhance protein adsorption and subsequent cell behavior on TZP.

The results obtained by this study should be confirmed by clarifying the relationship between surface wettability and cell adhesion, proliferation, differentiation, and matrix mineralization, in addition to protein adsorption on TZP surfaces. The findings of this study suggest that modification of either surface topography or physicochemistry greatly influences the surface wettability of TZP, possibly enhancing protein adsorption and subsequent cell behavior. This technology, then, has the potential to allow control of the surface of a TZP implant to facilitate osseointegration. Furthermore, the present results indicate that superhydrophilicity is maintained, even with storage in an aqueous solution after surface modification, an important consideration in a clinical setting.

CONCLUSIONS

The surface modification of surface topography or physicochemistry, especially of blast/acid etching as well as O_2 plasma treatment and UV treatment, greatly increased the surface wettability, resulting in superhydrophilicity. XPS revealed that a remarkable decrease in carbon content and the introduction of hydroxyl groups were responsible for the observed superhydrophilicity. Furthermore, superhydrophilicity was maintained, even after immersion in an aqueous solution, an important consideration in the clinical application of this technology.

ACKNOWLEDGMENT

The authors would like to thank Associate Professor Jeremy Williams for his assistance with the English of this article.

REFERENCES

1. Christel P, Meunier A, Heller M, Torre JP, Peille CN. Mechanical properties and short-term in-vivo evaluation of yttrium-oxide-partially-stabilized zirconia. J Biomed Mater Res 1989;23:45–61.
2. Piconi C, Maccauro G. Zirconia as a ceramic biomaterial. Biomaterials 1999;20:1–25.
3. Sennerby L, Dasmah A, Larsson B, Iverhed M. Bone tissue responses to surface modified zirconia implants: A histomorphometric and removal torque study in the rabbit. Clin Implant Dent Relat Res 2005;7:S13–S20.
4. Scarano A, Di Carlo F, Quaranta M, Piattelli A. Bone response to zirconia ceramic implants: An experimental study in rabbits. J Oral Implantol 2003;29:8–12.
5. Kohal RJ, Weng D, Bachle M, Strub JR. Loaded custom-made zirconia and titanium implants show similar osseointegration: An animal experiment. J Periodontol 2004;75:1262–1268.
6. Gahlert M, Gudehus T, Eichhorn S, Steinhauser E, Kniha H, Erhardt W. Biomechanical and histomorphometric comparison between zirconia implants with varying surface textures and a titanium implant in the maxilla of miniature pigs. Clin Oral Implants Res 2007;18:662–668.
7. Gahlert M, Roehling S, Sprecher CM, Kniha H, Milz S, Bormann, K. In vivo performance of zirconia and titanium implants: A histomorphometric study in mini pig maxillae. Clin Oral Implants Res 2012;23:281–286.
8. Depprich R, Zipprich H, Ommerborn M, Naujoks C, Handschel J, Wiesmann HP, Kubler NR, Meyer U. Osseointegration of zirconia implants compared with titanium: An in vivo study. Head Face Med 2008;4:1–8.
9. Kohal RJ, Baechle M, Han JS, Hueren D, Huebner U, Butz F. In vitro reaction of human osteoblasts on alumina-toughened zirconia. Clin Oral Implants Res 2009;20:1265–1271.
10. Bächle M, Butz F, Hübner U, Bakalinis E, Kohal RJ. Behaviour of CAL72 osteoblastlike cells on zirconia ceramics with different surface topographies. Clin Oral Implants Res 2007;18:53–59.
11. Yoshinari M, Matsuzaka K, Inoue T, Oda Y, Shimono M. Bio-functionalization of titanium surfaces for dental implants. Mater Trans 2002;43:2494–2501.
12. Yoshinari M, Matsuzaka K, Inoue T. Surface modification by cold-plasma technique for dental implants—Bio-functionalization with binding pharmaceuticals. Jpn Dent Sci Rev 2011;47:89–101.
13. Dewez JL, Doren A, Schneider YJ, Rouxhet PG. Competitive adsorption of proteins: Key of the relationship between substratum surface properties and adhesion of epithelial cells. Biomaterials 1999;20:547–559.
14. Wei J, Yoshinari M, Takemoto S, Hattori M, Kawada E, Liu B, Oda Y. Adhesion of mouse fibroblasts on hexamethyldisiloxane surfaces with wide range of wettability, J Biomed Mater Res B 2007; 81:66–75.
15. Wei J, Igarashi T, Okumori N, Igarashi T, Maetani T, Liu B, Yoshinari M. Influence of surface wettability on competitive protein adsorption and initial attachment of osteoblasts. Biomed Mater 2009;4:045002.
16. van Kooten TG, Spijker HT, Busscher HJ. Plasma-treated polystyrene surfaces: Model surfaces for studying cell–biomaterial interactions. Biomaterials 2004;25:1735–1747.
17. Att W, Takeuchi M, Suzuki T, Kubo K, Anpo M, Ogawa T. Enhanced osteoblast function on ultraviolet light-treated zirconia. Biomaterials 2009;30:1273–1280.
18. Sousa SR, Lamghari M, Sampaio P, Moradas-Ferreira P, Barbosa MA. Osteoblast adhesion and morphology on TiO_2 depends on the competitive preadsorption of albumin and fibronectin. J Biomed Mater Res A 2008;84:281–290.
19. Kasemo B, Lausmaa J. Biomaterial and implant surfaces: On the role of cleanliness, contamination, and preparation procedures. J Biomed Mater Res 1988;22:145–158.
20. Shibata Y, Hosaka M, Kawai H, Miyazaki T. Glow discharge plasma treatment of titanium plates enhances adhesion of osteoblast-like cells to the plates through the integrin-mediated mechanism. Int J Oral Maxillofac Implants 2002;17:771–777.
21. Park JH, Olivares-Navarrete R, Baier RE, Meyer AE, Tannenbaum R, Boyan BD, Schwartz Z. Effect of cleaning and sterilization on titanium implant surface properties and cellular response. Acta Biomater 2011 December 2 [Epub ahead of print].
22. Aita H, Hori N, Takeuchi M, Suzuki T, Yamada M, Anpo M, Ogawa T. The effect of ultraviolet functionalization of titanium on integration with bone. Biomaterials 2009;30:1015–1025.
23. Rupp F, Scheideler L, Olshanska N, de Wild M, Wieland M, Geis-Gerstorfer J. Enhancing surface free energy and hydrophilicity through chemical modification of microstructured titanium implant surfaces. J Biomed Mater Res 2006;76A:323–334.
24. Wennerberg A, Albrektsson T. Suggested guidelines for the topographic evaluation of implant surfaces. Int J Oral Maxillofac Implants 2000;15:331–344.
25. Wennerberg A, Albrektsson T. Effects of titanium surface topography on bone integration: A systematic review. Clin Oral Implants Res 2009;20:172–184.

26. Kilpadi DV, Lemons JE, Liu J, Raikar GN, Weimer JJ, Vohra Y. Cleaning and heat-treatment effects on unalloyed titanium implant surfaces. Int J Oral Maxillofac Implants 2000;15:219–230.
27. Att W, Hori N, Takeuchi M, Ouyang J, Yang Y, Anpo M, Ogawa T. Time-dependent degradation of titanium osteoconductivity: An implication of biological aging of implant materials. Biomaterials 2009;30:5352–5363.
28. Kohal RJ, Wolkewitz M, Mueller C. Alumina-reinforced zirconia implants: Survival rate and fracture strength in a masticatory simulation trial. Clin Oral Implants Res 2010;21:1345–1352.
29. Kirsten A, Begand S, Oberbach T, Telle R, Fischer H. Subcritical crack growth behavior of dispersion oxide ceramics. J Biomed Mater Res B 2010;95:202–206.
30. Kohorst P, Borchers L, Strempel J, Stiesch M, Hassel T, Bach FW, Hübsch C. Low-temperature degradation of different zirconia ceramics for dental applications. Acta Biomater 2012;8:1213–1220.
31. Chevalier J, Gremillard L, Deville S. Low-temperature degradation of zirconia and implications for biomedical implants. Annu Rev Mater Res 2007;37:1–32.
32. Cales B, Drouin MJ. Low-temperature aging of Y-TZP ceramics. J Am Ceram Soc 1999;82:2150–2154.
33. Kosmac T, Oblak C, Jevnikar P, Funduk N, Marion L. Strength and reliability of surface treated Y-TZP dental ceramics. J Biomed Mater Res 2000;53:304–313.
34. Pittayachawan P, McDonald A, Petrie A, Knowles JC. The biaxial flexural strength and fatigue property of Lava Y-TZP dental ceramic. Dent Mater 2007;23:1018–1029.
35. Zhang Y, Pajares A, Lawn BR. Fatigue and damage tolerance of Y-TZP ceramics in layered biomechanical systems. J Biomed Mater Res B 2004;71:166–171.
36. Feng X, Jiang L. Design and creation of superwetting/antiwetting surfaces. Adv Mater 2006;18:3063–3078.
37. Drelich J, Chibowski E. Superhydrophilic and superwetting surfaces: Definition and mechanisms of control. Langmuir 2010;26: 18621–18623.
38. Wenzel RN. Resistance of solid surfaces to wetting by water. Ind Eng Chem 1936;28:988–994.
39. Kim WJ, Kim S, Lee BS, Kim A, Ah CS, Huh C, Sung GY, Yun WS. Enhanced protein immobilization efficiency on a TiO_2 surface modified with a hydroxyl functional group. Langmuir 2009;25: 11692–11697.
40. Wang R, Hashimoto K, Fujishima A. Light-induced amphiphilic surfaces. Nature 1997;388:431–432.
41. Zubkov T, Stahl D, Thompson TL, Panayotov D, Diwald O, Yates JT. Ultraviolet light-induced hydrophilicity effect on TiO_2(110) (1×1). Dominant role of the photooxidation of adsorbed hydrocarbons causing wetting by water droplets. J Phys Chem B 2005; 109:15454–15462.
42. Takeuchi M, Sakamoto K, Martra G, Coluccia S, Anpo M. Mechanism of photoinduced superhydrophilicity on the TiO_2 photocatalyst surface. J Phys Chem B 2005;109:15422–15428.
43. Liu Z, Amiridis MD, Chen Y. Characterization of CuO supported on tetragonal ZrO_2 catalysts for N_2O decomposition to N_2. J Phys Chem B 2005;109:1251–1255.
44. Wang X, Yu JC, Chen Y, Wu L, Fu X. ZrO_2-modified mesoporous nanocrystalline TiO_2–xN_x as efficient visible light photocatalysts. Environ Sci Technol 2006;40:2369–2374.
45. Wu JM, Hayakawa S, Tsuru K, Osaka A. Porous titania films prepared from interactions of titanium with hydrogen peroxide solution. Scripta Mater 2002;46:101–106.
46. Takemoto S, Yamamoto T, Tsuru K, Hayakawa S, Osaka A, Takashima S. Platelet adhesion on titanium oxide gels: Effect of surface oxidation. Biomaterials 2004;25:3485–3492.
47. Boehm HP. Acidic and basic properties of hydroxylated metal oxides surface. Discuss Faraday Soc 1971;52:264–275.
48. Feng J, Weng BC, Yang SX, Zhang XD. Characterization of surface oxide films on titanium and adhesion of osteoblast. Biomaterials 2003;24:4663–4670.
49. Van Kooten TG, Schakenraad JM, Van der Mei HC, Busscher HJ. Influence of substratum wettability on the strength of adhesion of human fibroblasts. Biomaterials 1992;13:897–904.
50. Redey SA, Razzouk S, Rey C, Bernache-Assollant D, Leroy G, Nardin M, Cournot G. Osteoclast adhesion and activity on synthetic hydroxyapatite, carbonated and natural calcium carbonate: Relationship to surface energy. J Biomed Mater Res 1999;45:140–147.